DESY 94–044
March 1994

$\mathcal{O}(\alpha^2 L^2)$ radiative corrections to deep inelastic ep scattering for different kinematical variables

Johannes Blümlein

DESY–Institut für Hochenergiephysik, Zeuthen,
Platanenallee 6, D–15735 Zeuthen, Germany

Abstract

The QED radiative corrections are calculated in the leading log approximation up to $\mathcal{O}(\alpha^2)$ for different definitions of the kinematical variables using jet measurement, the 'mixed' variables, the double angle method, and a measurement based on θ_e and y_{JB}. Higher order contributions due to exponentiation of soft radiation are included.

1 Introduction

The measurement of deep inelastic *ep* scattering at HERA will allow to extend the kinematical range to $x \sim 10^{-4}$ and $Q^2 \sim \mathcal{O}(10^4)\,\mathrm{GeV}^2$ [1]. Because of differences in the detector response and resolution [2] different ways to measure the kinematical variables x, y and Q^2 have to be used to cover the full kinematical range. Furthermore, owing to the different properties of detectors the experiments H1 and ZEUS [3] apply different methods in measuring the kinematical variables.

The QED radiative corrections in $\mathcal{O}(\alpha)$ differ significantly for the various choices of kinematical variables as shown in [4]. This is due to the full (or partial) integration of the radiated photon's phase space for different kinematical situations according to the experimental requirements. As shown in explicit comparisons between complete and leading log calculations in $\mathcal{O}(\alpha)$ the results agree to the per cent level for the case of lepton measurement [5, 6], jet measurement [7, 8], and the case of mixed variables [7, 9] [1]. In part of the phase space the $\mathcal{O}(\alpha)$ corrections are sizeable. Therefore, it is necessary to calculate the 2nd order corrections to check whether the results obtained are numerically stable.

In this letter the $\mathcal{O}(\alpha^2)$ contributions are calculated in the leading log approximation for the case of jet measurement, mixed variables, the double angle method [11], and a measurement based on θ_e and $y_{Jacquet-Blondel} \equiv y_{JB}$ [2]. The latter two methods have been applied by the ZEUS collaboration recently in measuring the deep inelastic neutral current cross section [13]. Since the $\mathcal{O}(\alpha L)$ radiative corrections for these cases have not been given before the corresponding numerical results will be included also. Besides of the second order leading log corrections higher order corrections due to soft exponentiation are given.

2 $\mathcal{O}(\alpha^2 L^2)$ corrections

The relevant contributions arise from the set of all possible collinear configurations in the diagrams up to $\mathcal{O}(\alpha^2)$. They are associated with the 'massless' fermion lines ($m_e^2, m_q^2 \ll Q^2$). One may group the different processes into:

1. bremsstrahlung (diagrams 1a,b, figure 1)
2. e^+e^- pair creation (diagram 1c), and
3. $f\bar{f}$ pair production, $f = l^-, u, d, s, c, b$, (diagram 1d).

Among the possible configurations contributions due to initial state and final state radiation both from the lepton and quark lines emerge. Furthermore, the Compton scattering of a nearly real intermediary photon, emitted from a quark or proton line and scattered off the electron, [5] may be considered as a part of the radiative corrections. Since the experimental signature of the latter process consists of two nearly balanced electromagnetic showers accompanied by low hadronic activity near the beam pipe, these events are generally not included into the deep inelastic sample. On the other hand, they may be used to measure the proton structure

[1] Also the case of 'hadronic' variables was investigated [9, 10]. However, these variables are not accessible in deep inelastic scattering experiments.

[2] For leptonic variables these corrections have been calculated in [12].

functions at small x and Q^2 [14]. Because of the finite detector resolutions collinear final state radiation is hardly resolved and may be treated integrally [15] in the experimental measurement. Due to this also terms with both collinear initial and final state radiation do not emerge. The initial state radiation from the quark line can be summed using Altarelli–Parisi equations [16] with kernels modified due to the 1st and 2nd order QED corrections, which yields a modification of the parton distributions at the level of 1% [3].

Because of this, we will consider only the effect of initial state radiation in the following. For the scattering cross section up to $\mathcal{O}(\alpha^2)$ one thus obtains:

$$
\begin{aligned}
\frac{d^2\sigma}{dxdy} &= \frac{d^2\sigma^{(0)}}{dxdy} + \frac{d^2\sigma^{(1)}}{dxdy} + \frac{d^2\sigma^{(2)}}{dxdy} \\
\frac{d^2\sigma^{(1)}}{dxdy} &= \frac{\alpha}{2\pi} \ln\left(\frac{Q^2}{m_e^2}\right) \int_0^1 dz P_{ee}^{(1)}(z) \left\{ \theta(z-z_0)\mathcal{J}(x,y,z) \frac{d^2\sigma^{(0)}}{dxdy}\Big|_{x=\hat{x},y=\hat{y},s=\hat{s}} - \frac{d^2\sigma^{(0)}}{dxdy} \right\} \\
\frac{d^2\sigma^{(2)}}{dxdy} &= \frac{1}{2}\left[\frac{\alpha}{2\pi} \ln\left(\frac{Q^2}{m_e^2}\right)\right]^2 \int_0^1 dz P_{ee}^{(2,1)}(z) \left\{ \theta(z-z_0)\mathcal{J}(x,y,z) \frac{d^2\sigma^{(0)}}{dxdy}\Big|_{x=\hat{x},y=\hat{y},s=\hat{s}} - \frac{d^2\sigma^{(0)}}{dxdy} \right\} \\
&+ \left(\frac{\alpha}{2\pi}\right)^2 \int_{z_0}^1 dz \left\{ \ln^2\left(\frac{Q^2}{m_e^2}\right) P_{ee}^{(2,2)}(z) + \sum_{f=l,q} \ln^2\left(\frac{Q^2}{m_f^2}\right) P_{ee,f}^{(2,3)}(z) \right\} \mathcal{J}(x,y,z) \frac{d^2\sigma^{(0)}}{dxdy}\Big|_{x=\hat{x},y=\hat{y},s=\hat{s}}
\end{aligned}
\tag{1}
$$

using standard techniques known from QCD [4]. Here, $d^2\sigma^{(0)}/dxdy$ denotes the Born cross section for deep inelastic neutral or charged current ep reactions[5] (cf. e.g. (3,4) in [7]), and the Jacobian $\mathcal{J}$ is given by

$$
\mathcal{J}(x,y,z) = \begin{vmatrix} \partial\hat{x}/\partial x & \partial\hat{y}/\partial x \\ \partial\hat{x}/\partial y & \partial\hat{y}/\partial y \end{vmatrix} \tag{2}
$$

The shifted variables $\hat{x} \equiv \hat{Q}^2/\hat{y}\hat{s}$, $\hat{y}, \hat{Q}^2$, $\hat{s}$, and the lower bounds of z, z_0, are listed in table 1 for the different choices of measurement.

Both for the double angle method and the measurement based on θ_e and y_{JB}, the rescaled variables $\hat{x}$ and $\hat{Q}^2$ vanish for $z \to z_0$ (cf. table 1). If *no* futher cut is imposed this means that for both methods the radiative corrections are strongly influenced by the non–perturbative range $x, Q^2 \to 0$ in $d^2\sigma/dxdy$. In studies by the ZEUS collaboration, where these two methods have been applied, however, the cut

$$
2E_e = E_e'(1-\cos\theta_e) + E_J(1-\cos\theta_J) \geq \mathcal{A} \tag{3}
$$

on the reconstructed electron beam energy was imposed, choosing $\mathcal{A} = 35\,\mathrm{GeV}$. Here, $\theta_{e,J}$ denote the scattering angle of the electron and the jet angle, respectively, and E_e, E_e', E_J are the energies of the initial electron, scattered electron, and the jet in the laboratory frame. This cut yields $z_0 = \mathcal{A}/(2E_e)$ in the case of the double angle method and $z_0 = \max\{\mathcal{A}/(2E_e), y\}$

[3]Note, that the current uncertainty in the parton distributions is larger than this in most of the kinematical range [17]–[20].

[4]These methods have also been used for the calculation of QED corrections to e^+e^- annihilation processes successfully [21].

[5]Note, that QED loop effects, as e.g. the polarization of the intermediary boson, are not included in (1). One may easily account for them using 'dressed' Born cross sections instead of $d\sigma^{(0)}/dxdy$.

for the measurement based on θ_e and y_{JB}. For the double angle method the cut excludes the contributions of the range $x, Q^2 \to 0$ globally, whereas they are still present in the case of the $\theta_e - y_{JB}$ measurement for $\mathcal{A}/(2E_e) \lesssim y$.

The splitting functions in (1) are:

$$P_{ee}^{(1)}(z) = \frac{1+z^2}{1-z} \tag{4}$$

$$\begin{aligned} P_{ee}^{(2,1)}(z) &= \frac{1}{2}\left[P_{ee}^{(1)} \otimes P_{ee}^{(1)}\right](z) \\ &= \frac{1+z^2}{1-z}\left[2\ln(1-z) - \ln z + \frac{3}{2}\right] + \frac{1}{2}(1+z)\ln z - (1-z) \end{aligned} \tag{5}$$

$$\begin{aligned} P_{ee}^{(2,2)}(z) &= \frac{1}{2}\left[P_{e\gamma}^{(1)} \otimes P_{\gamma e}^{(1)}\right](z) \\ &\equiv (1+z)\ln z + \frac{1}{2}(1-z) + \frac{2}{3}\frac{1}{z}(1-z^3) \end{aligned} \tag{6}$$

$$P_{ee,f}^{(2,3)}(z) = N_c(f) e_f^2 \frac{1}{3} P_{ee}^{(1)}(z)\theta\left(1 - z - \frac{2m_f}{E_e}\right) \tag{7}$$

Here, $P_{e\gamma}^{(1)}$ and $P_{\gamma e}^{(1)}$ are the splitting functions of a photon into an electron, and vice versa. $\otimes$ denotes the Mellin convolution. e_f is the fermion charge, and $N_c(f) = 3$ for quarks, $N_c(f) = 1$ for leptons, respectively. (7) is obtained from an expansion of $\alpha_{QED}(s)$ calculating the polarization operator in the on–mass–shell scheme for leptons *and* quarks, which can not be done reliably in perturbative QCD in the case of the light quarks. However, one may try to *parametrize* $\alpha_{QED}(s, m_{f_i})$ in terms of *effective* quark masses from a fit to $R(s) = \sigma(e^+e^- \to \text{hadrons})/\sigma(e^+e^- \to \mu^+\mu^-)$ as done in [22]. We will apply this description here and use the parameters $m_u = 62\,\text{MeV}$, $m_d = 83\,\text{MeV}$, $m_s = 215\,\text{MeV}$, $m_c = 1.5\,\text{GeV}$, and $m_b = 4.5\,\text{GeV}$ as obtained in [22] in the subsequent analysis.

The soft exponentiation beyond the second order can be calculated using the solution of the non–singlet evolution equation for the electron or positron distribution in the soft range $(z \to 1)$ for running α_{QED}. It is given by [23]

$$D_{NS}(z, Q^2) = \zeta(1-z)^{\zeta-1} \frac{\exp\left[\frac{1}{2}\zeta\left(\frac{3}{2} - 2\gamma_E\right)\right]}{\Gamma(1+\zeta)} \tag{8}$$

with

$$\zeta = -3\ln\left[1 - (\alpha/3\pi)\ln(Q^2/m_e^2)\right] \tag{9}$$

Expanding (8) up to $\mathcal{O}(\alpha^2)$, one obtains terms in the limit $z \to 1$ which are contained in (1) already. Apart from bremsstrahlung terms also the e^+e^- pair production term in (7) is included for $m_e \to 0$ [6]. To account for the terms of $\mathcal{O}(\alpha^3)$ and higher orders contained in (8), we use

$$P_{ee}^{>2,\ soft}(z, Q^2) = D_{NS}(z, Q^2) - \frac{\alpha}{2\pi}\ln\left(\frac{Q^2}{m_e^2}\right)\frac{2}{1-z}\left\{1 + \frac{\alpha}{2\pi}\ln\left(\frac{Q^2}{m_e^2}\right)\left[\frac{11}{6} + 2\ln(1-z)\right]\right\} \tag{10}$$

[6] One might generalize (9) using also the heavier fermions $u, d, \mu, s, ...$ in the running coupling constant. However, apart from of the mass threshold in (7) the smaller logarithm associated with these terms will yield an even smaller contribution.

and[7]

$$\frac{d^2\sigma^{(>2,soft)}}{dxdy} = \int_0^1 dz P_{ee}^{(>2)}(z,Q^2)\left\{\theta(z-z_0)\mathcal{J}(x,y,z)\frac{d^2\sigma^{(0)}}{dxdy}|_{x=\hat{x},y=\hat{y},s=\hat{s}} - \frac{d^2\sigma^{(0)}}{dxdy}\right\} \tag{11}$$

Beginning with the second order corrections in α terms due to $e^- \rightarrow e^+$ conversion in the initial state contribute. They result from diagram 1c in $\mathcal{O}(\alpha^2)$ where now the outgoing fermion collinear with the incoming electron is a positron. The conversion rate equals

$$P(z,Q^2;e^- \rightarrow e^+) = \left(\frac{\alpha}{2\pi}\right)^2 \ln^2\left(\frac{Q^2}{m_e^2}\right) P_{ee}^{(2,2)}(z) \tag{12}$$

This quantity is illustrated in figure 2 numerically. For $Q^2 \gtrsim 10\,\mathrm{GeV}^2$, $P(z,Q^2;e^- \rightarrow e^+)$ may reach values of $\mathcal{O}(1)$ for $z \sim 10^{-4}$. Depending on the detector resolution the charge of the scattered lepton in deep inelastic ep collisions might only be measurable in part of the kinematical range. If the charge of the recorded final state electron is ignored in the measurement, also the contribution

$$\frac{d^2\sigma^{(2,e^-\rightarrow e^+)}}{dxdy} = \int_{z_0}^1 dz P(z,Q^2;e^- \rightarrow e^+)\mathcal{J}(x,y,z)\frac{d^2\sigma^{(0)}}{dxdy}|_{x=\hat{x},y=\hat{y},s=\hat{s}} \tag{13}$$

has to be included in the radiative corrections. The corresponding contributions are given for the different cases of measurement separately below.

3 Numerical results

In the numerical calculation the quark distributions are parametrized in the DIS scheme using the MRS D^- parton distributions [17] to illustrate the correction functions $\delta_i(x,y)$ for the different type of measurements. Equivalent results are obtained using the recent MRSH [18], CTEQ [19], or GRV [20] distributions.

The value of $\hat{Q}^2$ for the structure functions in the radiative orders in (1) may become smaller than the usual lower bound $Q_0^2 \sim 4\,\mathrm{GeV}^2$ for which the chosen parton parametrization applies. Because of Lorentz invariance the structure functions $F_{2,3}^i(x,Q^2)$ vanish with $Q^2 \rightarrow 0$. Various parametrizations of this behaviour have been proposed recently [24]. Here, for an illustration, we will adopt a multiplicative factor [25]

$$\times\left[1-\exp(-A^2\hat{Q}^2)\right] \quad \text{with} \quad A^2 = 3.37\,\mathrm{GeV}^{-2}. \tag{14}$$

for all structure functions in the numerical calculations.

Figure 3 illustrates the $\mathcal{O}(\alpha^2 L^2)$ corrections for the case of jet measurement for neutral current deep inelastic e^-p scattering. The corrections are positive and grow with x and y. Compared with the 1st order results [7] they diminish the negative $\mathcal{O}(\alpha)$ results in size. In the low x range $x \lesssim 0.01$ the 2nd order corrections are found to be less than 1 %. Still smaller values are found for the 2nd order contribution due to $e^- \rightarrow e^+$ conversion, which amount to relative corrections $< 4 \cdot 10^{-4}$ only.

[7]To obtain consistency between eqs. (10) and (1) the limit $m_e \rightarrow 0$ in (7) is taken.

The 2nd order corrections for jet measurement in the case of charged current deep inelastic $e^- p$ scattering are the same as those of the corresponding neutral current reactions for large x, because this range is dominated by the soft and virtual contributions, cf. figure 4. For smaller values of $x \lesssim 0.01$ they are smaller than 1 % and may become negative, as also the 1st order corrections change sign for small x [7]. The contributions due to $e^- \rightarrow e^+$ conversion are somewhat larger than in the case of neutral current reactions.

For the measurement based on mixed variables, i.e. Q^2 measured at the leptonic and y_{JB} at the hadronic vertex (see figure 5), the 2nd order corrections to the neutral current cross section turn out to be less than 1 % in the range $y \gtrsim 0.2$. They become smaller with descending x values. For $x \sim 0.5$ they reach 10 % in the range of small y. Note that contrary to the jet measurement the contributions due to $e^- \rightarrow e^+$ conversion become of comparable order as the 2nd order $e^- \rightarrow e^-$ corrections for small y in the case of mixed variables.

The $\mathcal{O}(\alpha)$ and $\mathcal{O}(\alpha^2)$ corrections for the neutral current deep inelastic scattering cross section for a measurement using the double angle method are shown in figure 6. Both the 1st and 2nd order corrections are nearly flat in y. The corrections become smaller with descending values of x and are smaller than 3 % for $x \lesssim 0.01$. Due to these properties the double angle method appears to be an ideal choice to measure the neutral current cross section from the point of view of radiative corrections. The contributions from $e^- \rightarrow e^+$ conversion are less than $2 \cdot 10^{-4}$.

Figure 7 shows the $\mathcal{O}(\alpha)$ and $\mathcal{O}(\alpha^2)$ corrections for the neutral current deep inelastic scattering cross section, where the scattering angle θ_e of the electron ond y_{JB} are used to define the kinematical variables. In this case the corrections grow rapidly in the range $y \approx \mathcal{A}/(2E_e)$ and become larger than 100 % for $y \gtrsim \mathcal{A}/(2E_e)$ already for $x = 0.01$. Even larger corrections are obtained for higher x values. This is caused by the shift of the rescaled variables $\hat{x} \rightarrow 0$ and $\hat{Q}^2 \rightarrow 0$ in the vicinity of $z_0 \approx y$. The relative correction becomes smaller for very low values of x, since the differential cross sections at the rescaled variables and the non-rescaled variables become less different in value there. The 2nd order corrections are negative. The contributions due to $e^- \rightarrow e^+$ conversion grow with rising values of x and amount to $\mathcal{O}(2\%)$ of the Born cross section for $x \sim 0.5$ and larger values of y. Because in part of the kinematical range the correction $\delta_{NC}(x, y)$ is significantly influenced by the behaviour of $d\sigma^{(0)}/dxdy$ in the non–perturbative range, a reliable calculation of $\delta_{NC}(x, y)$ is only possible knowing the behaviour $d\sigma^{(0)}/dxdy$ in the range of $Q^2, x \rightarrow 0$. Due to this the plot of $\delta_{NC}(x, y)$ in figure 7 serves only to show the *principal* behaviour under some assumptions made for $d\sigma^{(0)}/dxdy$. If, on the other hand, the cross section $d\sigma/dxdy$, which includes the radiative corrections, is well understood with respect to the experimental systematics, one may later try to use the measurement based on θ_e and y_{JB} as a method to unfold $d\sigma^{(0)}/dxdy$ in the non–perturbative range.

In summary, we found that the $\mathcal{O}(\alpha^2 L^2)$ corrections, supplemented by the soft exponentiation, for the neutral and charged current deep inelastic ep scattering cross sections amount to $\lesssim 10\%$ for the cases of jet measurement, mixed variables, and the double angle method. These contributions are of the order of the difference between the complete $\mathcal{O}(\alpha)$ and the leading log result $\mathcal{O}(\alpha L)$. In the case of the measurement based on θ_e and y_{JB}, contributions from the non–perturbative range $x, Q^2 \rightarrow 0$ influence both the 1st and 2nd order corrections.

Acknowledgement. I would like to thank Paul Söding for reading the manuscript.

References

[1] J. Blümlein, J. Feltesse, and M. Klein, in: Proc. of the ECFA Large Hadron Collider Workshop, Aachen 1990, eds. G. Jarlskog and D. Rein, Vol. **2** (CERN, Geneva, 1991), p. 830, CERN 90–10, ECFA 90–133;
M. Klein, in: Proc. of the 1991 HERA Physics Workshop, eds. W. Buchmüller and G. Ingelman, Vol. **1**, p. 71.

[2] J. Blümlein and M. Klein, Nucl. Instr. Meth. **A329** (1993) 112.

[3] M. Derrick et al., ZEUS collaboration, Phys. Lett. **B316** (1993) 412;
I. Abt et al., H1 collaboration, Nucl. Phys. **B407** (1993) 515.

[4] for a recent review see: H. Spiesberger, et al., in: Proc. of the 1991 HERA Physics Workshop, eds. W. Buchmüller and G. Ingelman, Vol. **2**, p. 798, and references therein.

[5] W. Beenakker, F. Berends, and W. van Neerven, Proceedings of the Ringberg Workshop 1989, ed. J.H. Kühn, (Springer, Berlin, 1989), p. 3;
J. Blümlein, Z. Phys. **C47** (1990) 89.

[6] D. Bardin, C. Burdik, P. Christova, and T. Riemann, Z. Physik, **C42** (1989) 679;
M. Böhm and H. Spiesberger, Nucl. Phys. **B294** (1987) 1081; H. Spiesberger, DESY 89–175.

[7] J. Blümlein, Phys. Lett. **B271** (1991) 267.

[8] A. Akhundov, D. Bardin, L. Kalinovskaya, and T. Riemann, Phys. Lett. **B301** (1993) 447.

[9] A. Akhundov, D. Bardin, L. Kalinovskaya, and T. Riemann, TERAD91–2.10, in: Proc. of the 1991 HERA Physics Workshop, eds. W. Buchmüller and G. Ingelman, Vol. **3**, p. 1285.

[10] H. Spiesberger, EPRC91, see [4].

[11] S. Bentvelsen, J. Engelen, and P. Kooijman, in: Proc. of the 1991 HERA Physics Workshop, eds. W. Buchmüller and G. Ingelman, Vol. **1**, p. 23.

[12] E.A. Kuraev, N.P. Merenkov, and V.S. Fadin, Sov. J. Nucl. Phys. **47** (1988) 1009;
J. Kripfganz, H.–J. Möhring, and H. Spiesberger, Z. Phys. **C 49** (1991) 501.

[13] S. Schlenstedt, priv. communication.

[14] J. Blümlein, G. Levman, and H. Spiesberger, in: Proc. 'Research Directions of the Decade', Snowmass, 1990, ed. E.L. Berger, (World Scientific, Singapore, 1992) p. 554; J. Phys. **G19** (1993) 1695.

[15] T. Kinoshita, J. Math. Phys. **B271** (1991) 267;
T.D. Lee and M. Nauenberg, Phys. Rev. **133** (1964) B1549.

[16] A. De Rujula, R. Petronzio, and A. Savoy–Navarro, Nucl. Phys. **B154** (1979) 394.

[17] A.D. Martin, W.J. Stirling, and R.G. Roberts, Phys. Lett. **B306** (1993) 145; Erratum: ibid. **B309** (1993) 492.

[18] A.D. Martin, W.J. Stirling, and R.G. Roberts, Durham preprint DTP–93–86, Oct. 1993.

[19] J. Botts, J. Morfin, J. Owens, J. Qiu, W. Tung, and H. Weerts, CTEQ collaboration, East Lansing preprint MSU–HEP 93/18 (1993).

[20] M. Glück, E. Reya, and A. Vogt, Z. Phys. **C48** (1990) 401.

[21] E.A. Kuraev and V.S. Fadin, Sov. J. Nucl. Phys. **41** (1985) 466;
G. Altarelli and G. Martinelli, CERN Yellow Report 86–02, Vol. **1**, p. 47;
W. Beenakker et al. [5];
O. Nicrosini and L.Trentadue, Phys. Lett. **B196** (1987) 551;
G. Montagna, O. Nicrosini, and L. Trentadue, Phys. Lett. **B231** (1989) 492;
M. Cacciari, A. Deandrea, G. Montagna, O. Nicrosini, and L. Trentadue, Phys. Lett. **B268** (1991) 441.

[22] F. Jegerlehner, preprint PSI–PR–91–08, Lectures at the Theoretical Advanced Study Institute in Elementary Particle Physics (TASI), Boulder, CO, 1990, Boulder TASI 90, p. 476–590.

[23] V. Gribov and L. Lipatov, Sov. J. Nucl. Phys. **15** (1972) 451, 675.

[24] For a comparison of these parametrizations see: B. Badelek et al., J. Phys. **G19** (1993) 1671, and references therein.

[25] N.Y. Volkonsky and L.V. Prokhorov, JETF Lett. **21** (1975) 389.

	$\hat{s}$	$\hat{Q}^2$	$\hat{y}$	z_0	$\mathcal{J}(x,y,z)$
jet measurement	zs	$Q^2(1-y)/(1-y/z)$	y/z	$y/[1-x(1-y)]$	$(1-y)/(z-y)$
mixed variables	zs	Q^2z	y/z	y	1
double angle method	zs	Q^2z^2	y	0	z
y_{JB} and θ_e	zs	$Q^2z(z-y)/(1-y)$	y/z	y	$(z-y)/(1-y)$

Table 1: Description of parameters in eq. (1) for different types of cross section measurement

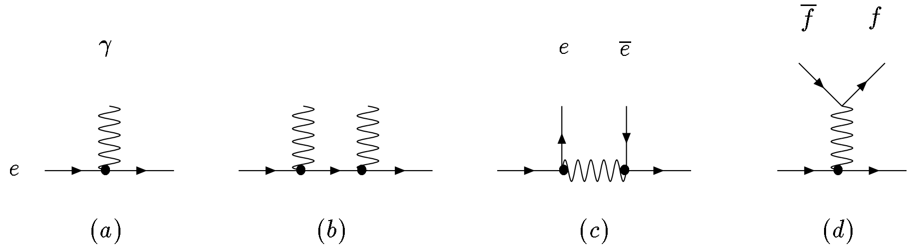

Figure 1: Diagrams contributing to the radiative corrections up to $\mathcal{O}(\alpha^2 L^2)$.

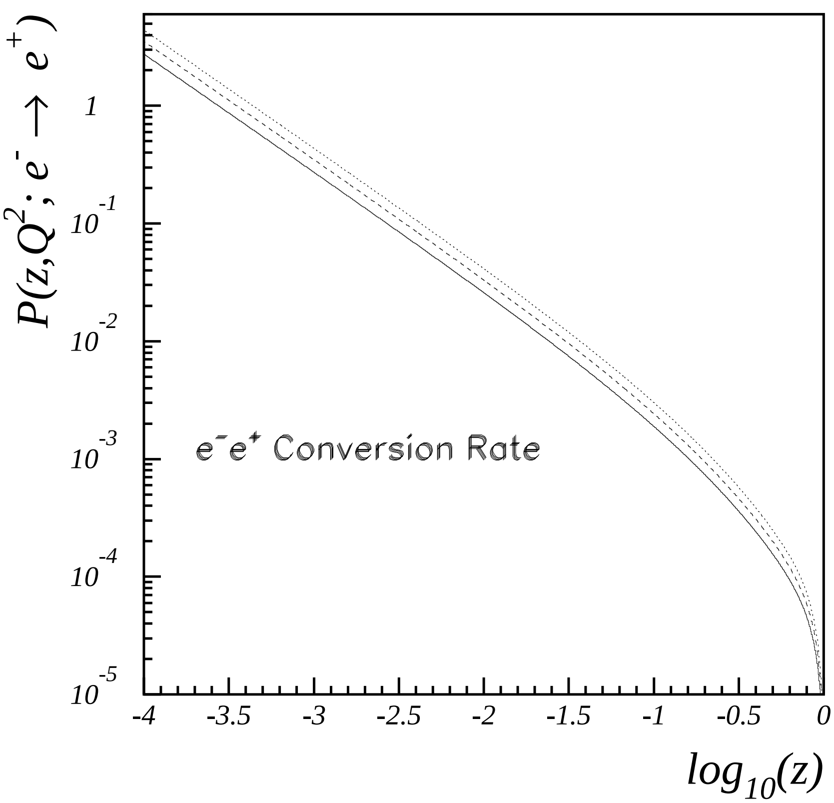

Figure 2: $e^- \rightarrow e^+$ transition rate for different values of Q^2. Full line: $Q^2 = 10\,\mathrm{GeV}^2$, dashed line: $Q^2 = 100\,\mathrm{GeV}^2$, and dotted line: $Q^2 = 1000\,\mathrm{GeV}^2$.

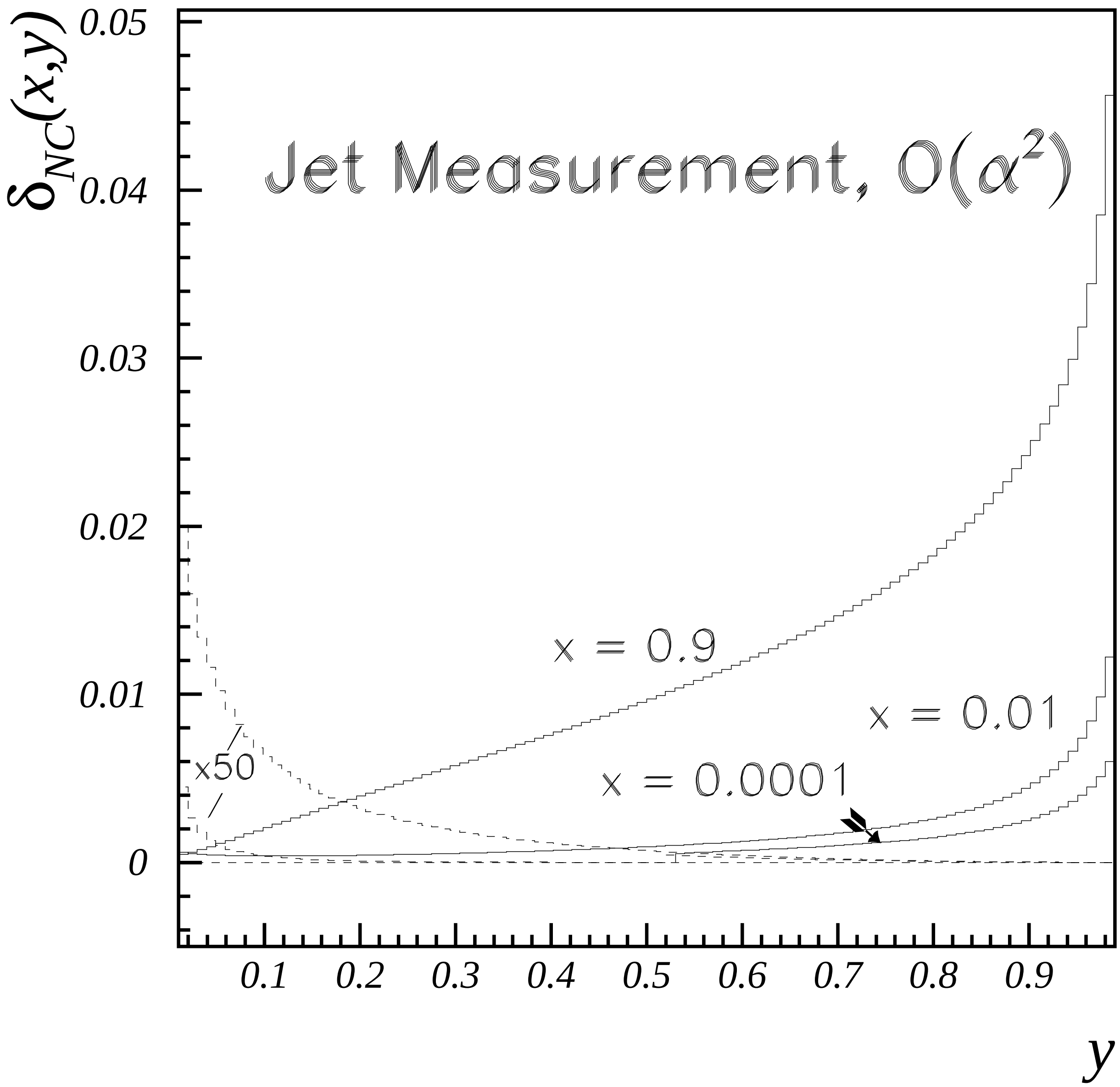

Figure 3: Leptonic initial state radiative corrections $\delta_{NC}(x,y) = (d\sigma^{(2+>2,soft)}/dxdy)/(d\sigma^0/dxdy)$ in LLA for e^-p deep inelastic scattering in the case of jet measurement for $\sqrt{s} = 314\,\mathrm{GeV}$, $\mathcal{A} = 0$, and $Q^2 \geq 5\,\mathrm{GeV}^2$. Full lines: $\mathcal{O}(\alpha^2)$ corrections. Dashed lines: contributions due to $e^- \to e^+$ conversion eq. (13), $\delta_{NC}^{e^-\to e^+}(x,y) = (d\sigma^{(2,e^-\to e^+)}/dxdy)/(d\sigma^0/dxdy)$ scaled by $\times 50$; upper line: $x = 0.01$, middle line: $x = 0.0001$, lower line $x = 0.9$.

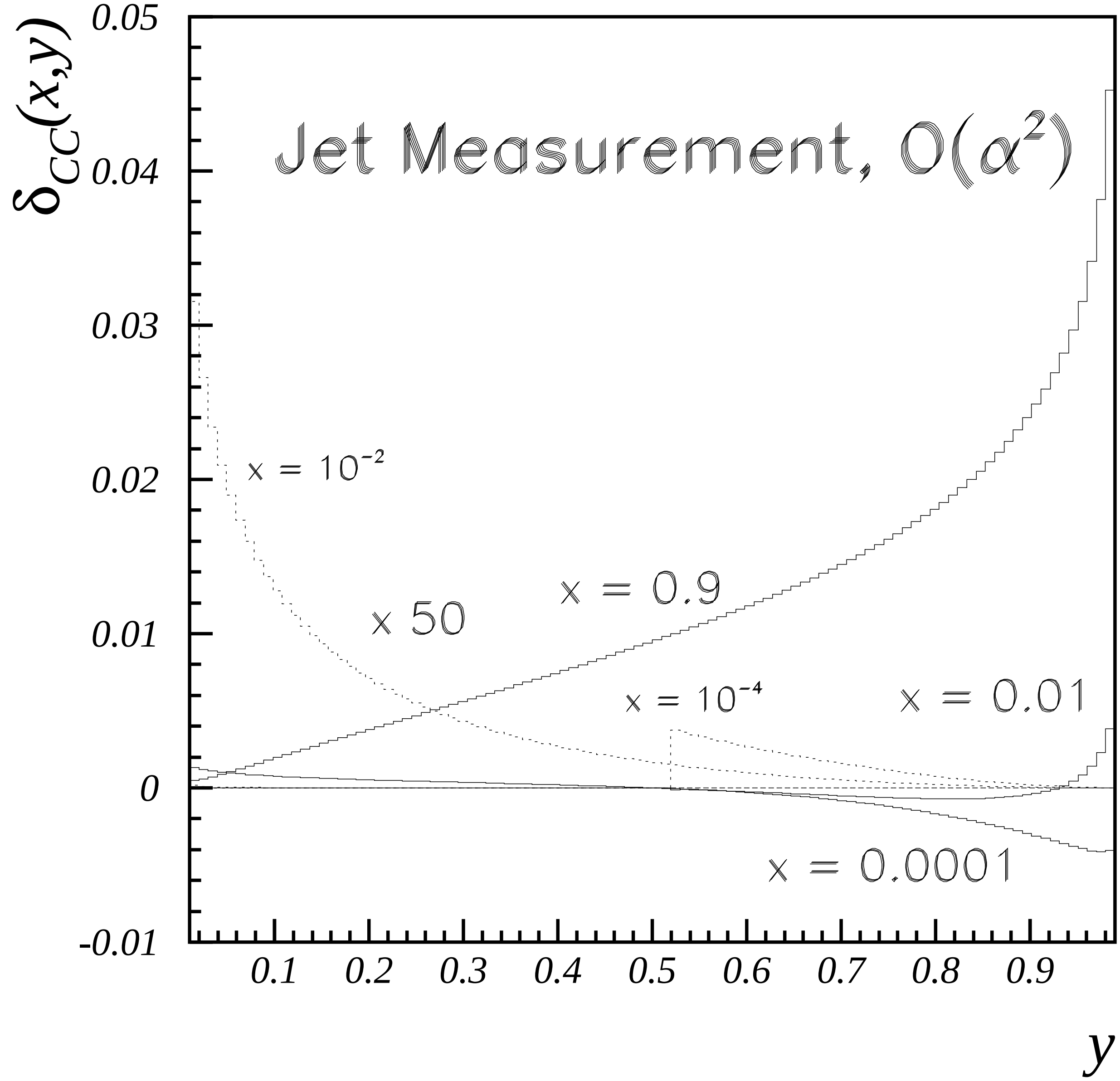

Figure 4: $\delta_{CC}(x,y) = (d\sigma_{CC}^{(2+>2,soft)}/dxdy)/(d\sigma_{CC}^{0}/dxdy)$ for deep inelastic e^-p scattering in the case of jet measurement. Dotted lines: $\delta_{CC}^{e^- \to e^+}(x,y)$. The other parameters are the same as in figure 3.

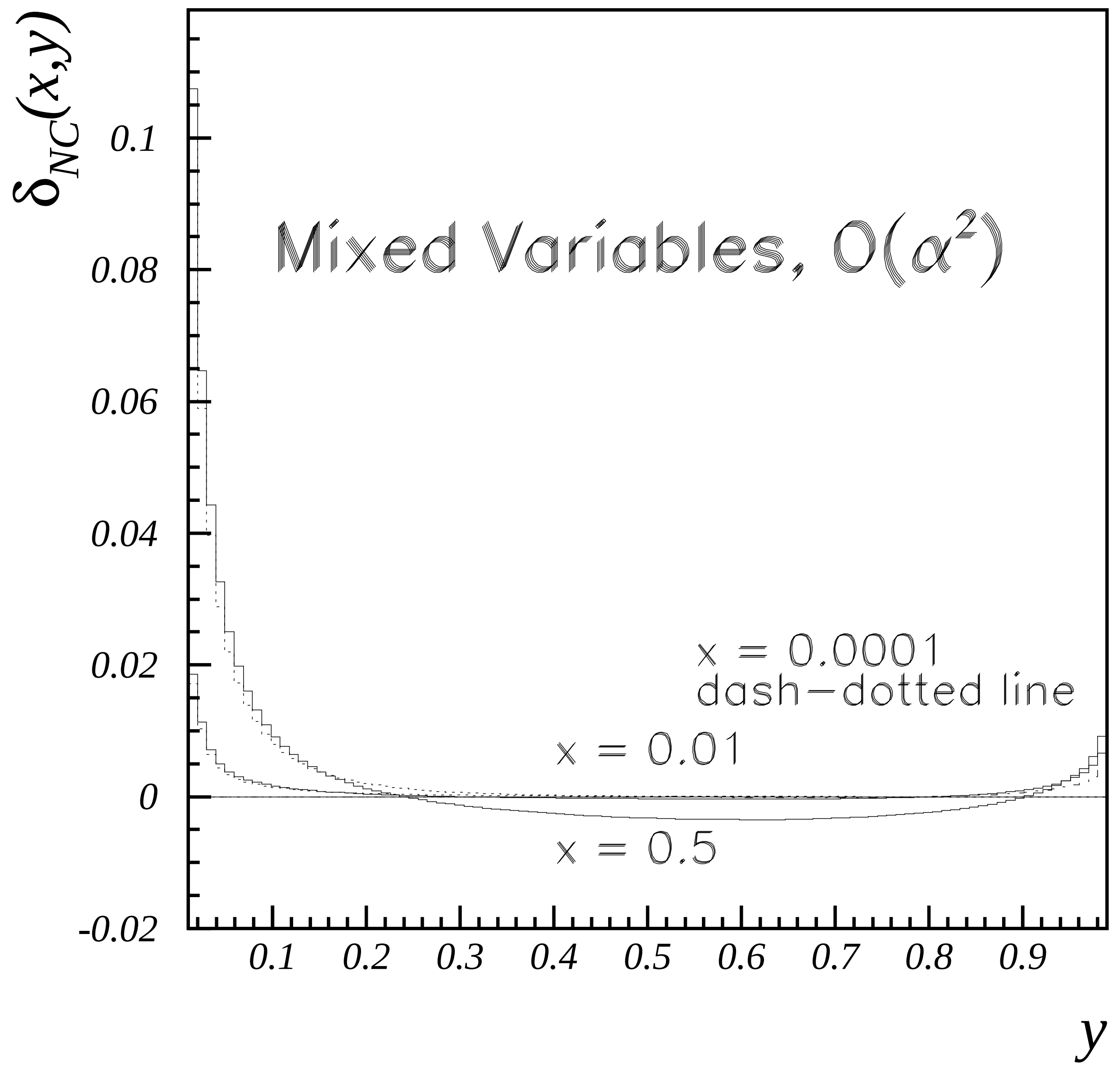

Figure 5: $\delta_{NC}(x, y)$ for the case of mixed variables. Dotted lines: $\delta_{NC}^{e^- \to e^+}(x, y)$; upper line: $x = 0.5$, lower line $x = 0.01$. The other parameters are the same as in figure 3.

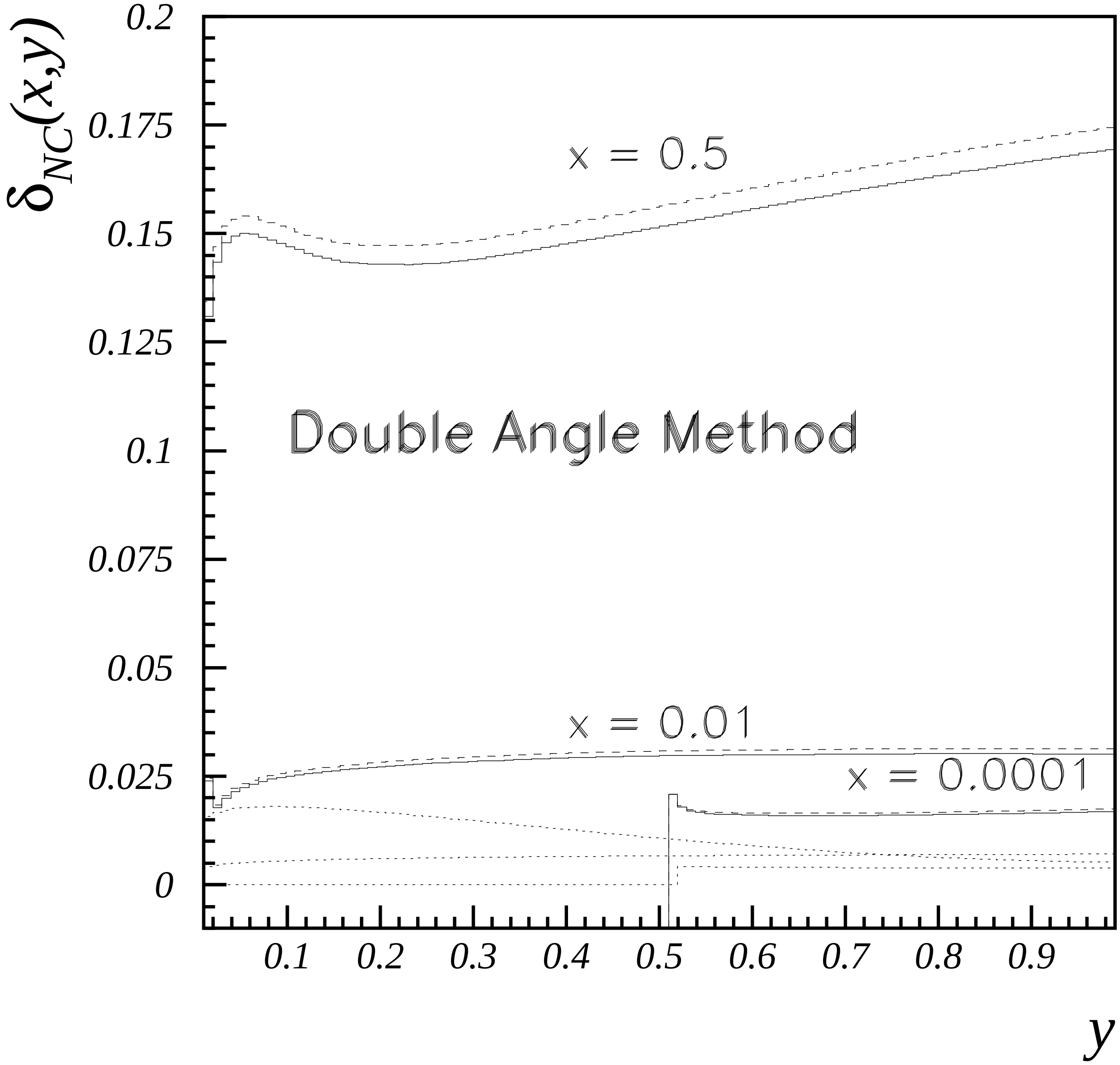

Figure 6: $\delta_{NC}(x,y)$ for the case of the double angle method for $\mathcal{A} = 35\,\mathrm{GeV}$. Full lines: $\delta_{NC}^{(1+2+>2,soft)}(x,y)$, dashed lines: $\delta_{NC}^{(1)}(x,y)$. Dotted lines: $\delta_{NC}^{e^-\to e^+}(x,y)$ scaled by $\times 100$; upper line: $x = 0.5$, middle line: $x = 0.01$, lower line: $x = 0.0001$. The other parameters are the same as in figure 3.

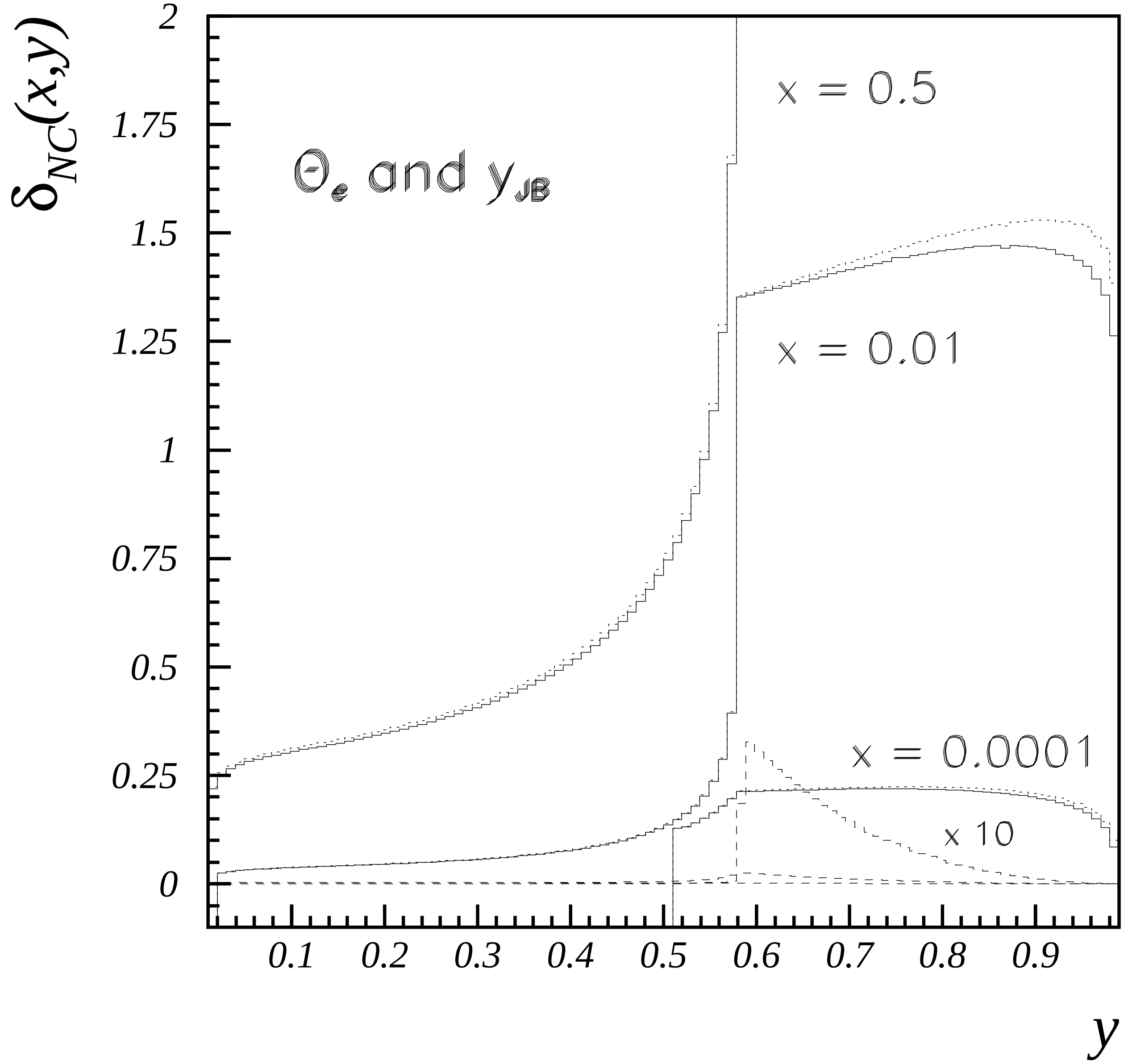

Figure 7: $\delta_{NC}(x,y)$ for the measurement based on θ_e and y_{JB} for $\mathcal{A} = 35\,\mathrm{GeV}$. Full lines: $\delta_{NC}^{(1+2+>2,soft)}(x,y)$, dotted lines: $\delta_{NC}^{(1)}(x,y)$. Dashed lines: $\delta_{NC}^{e^-\to e^+}(x,y)$; upper line: $x = 0.5$, middle line: $x = 10^{-2}$, lower line: $x = 10^{-4}$. The other parameters are the same as in figure 3.